Electronic Structure of Lithium Nickel Oxides by Electron Energy Loss Spectroscopy

Yukinori Koyama,*,† Teruyasu Mizoguchi,‡ Hidekazu Ikeno,§ and Isao Tanaka§

Department of Materials Science and Engineering, Nagoya University, Furo, Chikusa, Nagoya 464-8603, Japan, Institute of Engineering Innovation, The University of Tokyo, Yayoi, Bunkyo, Tokyo 113-8656, Japan, and Department of Materials Science and Engineering, Kyoto University, Yoshida, Sakyo, Kyoto 606-8501, Japan

Received: January 27, 2005

The electronic structures of NiO, $LiNiO_2$, and NiO_2 are studied by the electron energy loss spectroscopy at Ni $L_{2,3}$, Ni $M_{2,3}$, and O K edges. The Ni $L_{2,3}$ edge spectra suggest that the formal charge of nickel is +2 in NiO, +3 with a low-spin state in $LiNiO_2$, and +4 with a low-spin state in NiO_2. This is well confirmed by first-principles calculations. The Ni $M_{2,3}$ edge spectra show similar chemical shifts to those of the Ni $L_{2,3}$ edge. Superposition of the Li K edge spectrum, however, hinders further analysis. Although the formal charge of oxygen is −2 in all the three phases, the O K edge spectra indicate a more remarkable difference in the electronic structure of the oxygen in NiO_2 than that in either NiO or $LiNiO_2$. The spectra suggest that lithium extraction from $LiNiO_2$ reinforces the covalent bonding between the oxygen and nickel atoms and causes a notable reduction in electron density at the oxygen atoms.

Introduction

Transition-metal oxides that can electrochemically accommodate and release lithium ions are studied as electrode materials for lithium batteries. Historically, electrode materials have been searched for in an empirical way. First-principles calculation is a useful technique today to predict and understand fundamental properties of solid-state redox reactions.[1−12] However, it is not fully understood how the electronic structures of the transition-metal oxides are changed by insertion/extraction of a lithium ion and an electron. The conventional chemical idea assumes that lithium and oxygen atoms are ionized in oxides as Li^+ and O^{2-} ions, respectively. The charge of transition-metal atoms is so determined to follow charge neutrality. Consequently, insertion/extraction of a lithium ion simply changes the charge of the transition-metal atoms. For example, $LiNiO_2$ is regarded as an assemblage of Li^+, Ni^{3+}, and O^{2-} ions. Further lithium extraction to NiO_2 automatically leads to the formation of Ni^{4+} assuming the formal charge of O^{2-}. This description, however, lacks information on the local electronic structure. First-principles calculations provide more detailed information on the changes in the electronic structures associated with lithium insertion/extraction. Formal charges, which are derived from electronic configurations neglecting covalency, are the same as the expected values by the conventional chemical idea. Charge density distribution maps depicted by the first-principles calculations show that lithium extraction reduces electron density at oxygen atoms as well as at transition-metal atoms.[2,3,7,8,10,12] This predicts that the oxygen atoms also participate in the solid-state redox reactions associated with lithium insertion/extraction in the lithium transition-metal oxides.

Spectroscopic techniques are used for the experimental investigation on electronic structures. Near-edge X-ray absorption fine structure (NEXAFS) is one of these techniques. Ni K edge NEXAFS has been observed in NiO, $LiNiO_2$, and Li_xNiO_2 ($0 \le x < 1$).[13−17] It has been discussed that the chemical shifts of the Ni K edge indicate that nickel atoms are in different charge states among the phases. Despite the clear difference in the chemical shift, Ni K is not an optimum edge to study the electronic structures around the Fermi level. Ni-3d and O-2p orbitals construct the electronic structures around the Fermi level in the phases, but the electric-dipole selection rule does not allow electron transitions from a Ni-1s core level to these orbitals. Hence, the Ni K edge NEXAFS provides only indirect information on the electronic structures around the Fermi level. The Ni $L_{2,3}$ and O K edge spectra should be more informative. They, respectively, correspond to transitions from Ni-2p to Ni-3d and from O-1s to O-2p. It has been reported that the Ni $L_{2,3}$ edge spectra of $LiNiO_2$ and $LiCo_yNi_{1-y}O_2$ ($0 < y < 1$) are similar to that of NiO.[18,19] Accordingly, it is suggested that the formal charge of nickel is +2 even in these phases. Carefulness is necessary to rely on the soft X-ray NEXAFS obtained by the electron yield method, since the spectra are generally very sensitive to surface states. Therefore, another method that is less sensitive to surface states should be applied to verify the electronic structures for the bulk.

In this paper, the electronic structures of NiO, $LiNiO_2$, and NiO_2 are studied by the electron energy loss spectroscopy (EELS) to understand the solid-state redox reaction of $LiNiO_2$ from the viewpoint of the electronic structure. Energy loss is measured for individual electrons passing through a specimen by transmission electron microscopy (TEM). Since the transitions of core electrons basically follow the electric-dipole selection rule, a core-loss spectrum in EELS, electron energy loss near-edge structure (ELNES), is similar to NEXAFS. ELNES can be measured on selected particles or areas simultaneously with TEM observation. This is an advantage of ELNES when the sample contains multiple phases. NEXAFS

* Corresponding author. Address: Massachusetts Institute of Technology, 77 Massachusetts Avenue, Room 13-4038, Cambridge, MA 02139-4307; phone: +1-617-253-6891; fax: +1-617-253-6201; e-mail: koyamay@MIT.EDU.

† Nagoya University.

‡ The University of Tokyo.

§ Kyoto University.

10.1021/jp050486b CCC: $30.25
Published on Web 04/30/2005

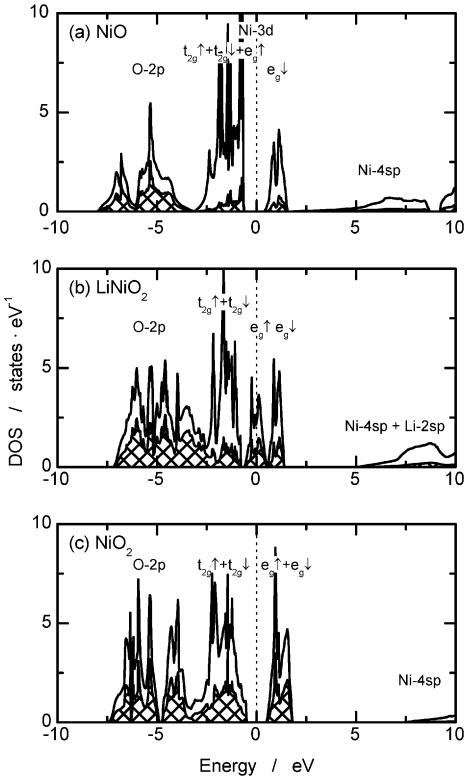

Figure 1. Density of states calculated for (a) NiO, (b) $LiNiO_2$, and (c) NiO_2. The figures are aligned so that Fermi energy is zero. Contribution of O-2p orbital is also shown in each figure by cross-patterned areas.

provides only the sum of the spectra from all the phases in the sample because of its poor spatial resolution. Moreover, ELNES is less sensitive to surface states than NEXAFS since only transmitted electrons are measured. Therefore, ELNES is a powerful and complementary experimental technique to NEXAFS.[17,20−22]

Electronic Structure of Nickel Oxides by First-Principles Calculation

Electronic structures of NiO, $LiNiO_2$, and NiO_2 by first-principles calculations are briefly shown in this section for easy understanding of EELS results in the present work. First-principles calculations on lithium transition-metal oxides have already been reported in the literature.[1−12] In the present work, electronic structures were calculated by the full-potential augmented plane-wave plus local orbitals (APW+lo) method using WIEN2k code.[23] The exchange-correlation interaction was considered within the generalized gradient approximation with spin-polarization. Antiferromagnetic spin ordering was adopted to NiO, while ferromagnetic spin ordering was applied to $LiNiO_2$ and NiO_2 for simplicity. An atomic spherical radius of 0.90 Å was used for all atoms. The number of basis functions was determined by an energy cutoff of 300 eV. Integration in the reciprocal space was done by the tetrahedron method with 65 sampling points in the irreducible Brillouin zone. Li-1s, Ni-3s, and Ni-3p orbitals were treated as semicore states.

The density of states around the Fermi energy is illustrated in Figure 1. A band located at −8 to −3 eV mainly consists of O-2p orbitals and the band is fully filled in all the three phases. Hence, oxygen atoms can be considered as O^{2-} ions in terms of the formal charge. Bands in a rage of −3 to +2 eV mainly consist of Ni-3d orbitals. Since nickel atoms are located at an octahedral position in the phases, the Ni-3d band is split into

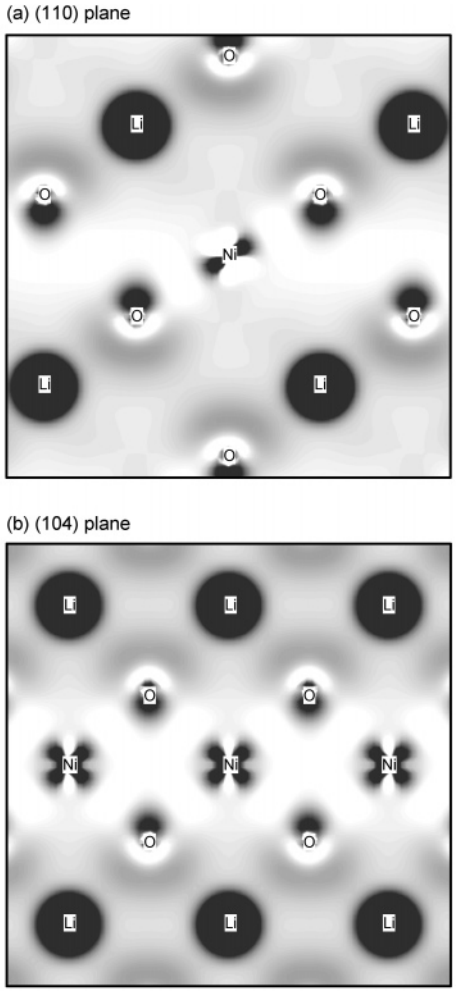

Figure 2. Difference in electron density distribution between $LiNiO_2$ and NiO_2 (a) on a (1 1 0) plane and (b) on a (1 0 4) plane. Position of each atom is also shown in the figures. Darker area indicates greater decrease in electron density by lithium extraction.

so-called t_{2g} and e_g bands with a spin up or down state. The other band above the Ni-e_g band mainly consists of Ni-4sp and Li-2sp orbitals, and the band is completely unoccupied. Observation of DOS tells that the electronic configuration of nickel is $(t_{2g}\uparrow)^3(t_{2g}\downarrow)^3(e_g\uparrow)^2$ in NiO, where ↑ and ↓, respectively, denote major and minor spins. The electronic configuration corresponds to the formal charge of Ni^{2+}. The electronic configuration is $(t_{2g}\uparrow)^3(t_{2g}\downarrow)^3(e_g\uparrow)^1$, which corresponds to Ni^{3+} with a low-spin state, in $LiNiO_2$, and $(t_{2g}\uparrow)^3(t_{2g}\downarrow)^3$, which corresponds to Ni^{4+} with a low-spin state, in NiO_2. Consequently, lithium extraction from $LiNiO_2$ to NiO_2 brings about the extraction of an electron from the Ni-$e_g\uparrow$ band as described by the conventional chemical sense. However, this describes only the formal charge. It does not include any information on the change in the local electronic structure.

Difference in charge density distribution between $LiNiO_2$ and NiO_2 was calculated as shown in Figure 2 to observe the details of the change in the electronic structure in the real space. The charge distribution of NiO_2 was calculated with the same structural parameters as those of $LiNiO_2$. A decrease in charge density by lithium extraction can be seen at the nickel atoms toward the neighboring oxygen atoms. This is due to the extraction of an electron from the Ni-$e_g\uparrow$ band, which corresponds to a σ-type bonding between the nickel and oxygen atoms. In addition to the decrease at the nickel atoms, a notable decrease can be seen at the oxygen atoms. This indicates that

the oxygen atoms participate in the solid-state redox reaction of $LiNiO_2$. The participation of the oxygen atoms can also be seen in the DOS, where the contribution of the O-2p orbitals in the Ni-3d band increases with lithium extraction. The contribution of the O-2p orbitals is actually very close to that of the Ni-3d in all the bands around the Fermi level in NiO_2.

Experimental Section

$LiNiO_2$ was prepared by a solid-state method.[24] A pellet of well-mixed $LiNO_3$ and $NiCO_3$ (1.07:1.00 in mole) was dried at 150 °C for 2 h and heated at 600 °C for 16 h. The pellet was ground and pressed into a pellet again. Then, the pellet was heated at 750 °C for 16 h. All the heat treatments were done in an oxygen stream. The prepared $LiNiO_2$ was characterized by X-ray diffraction (XRD) using a Cu Kα radiation with a graphite monochromator. The electrochemical activity of the sample was examined using a nonaqueous lithium cell. The positive electrode used in the cell was a mixture of 88% $LiNiO_2$, 6% acetylene black, and 6% polyvinylidene fluoride (PVdF) by weight. The negative electrode used was lithium on a stainless plate. The separator was two sheets of porous polypropylene membranes (Celgard 2500, Celgard Inc.). The electrolyte was 1 M $LiPF_6$ dissolved in a mixed solvent of ethylene carbonate (EC) and dimethyl carbonate (DMC) (3:7 by volume). Charge-discharge cycle tests were done with a constant current of 0.17 mA/cm^2 (12 mA/g by weight of $LiNiO_2$) in a range of 2.5−5.0 V at 30 °C.

NiO_2 was prepared by an electrochemical lithium extraction using a nonaqueous lithium cell. The cell consisted of a pellet of $LiNiO_2$ (about 40 mg in weight and 1.0 cm^2 in area), a lithium electrode, two sheets of the porous polypropylene membranes, and electrolyte as described above. No agent such as acetylene black or PVdF was added into the $LiNiO_2$ pellet to eliminate artifacts in EELS measurements. The cell was charged up to 5.0 V by a constant current of 0.1 mA/cm^2 (2.6 mA/g by weight of $LiNiO_2$). The charged cell was disassembled in a glovebox filled with argon and the pellet was rinsed with DMC to remove residual $LiPF_6$ salt. The sample was kept in DMC in a sealed bottle filled with argon until EELS measurements. The sample was exposed to air for 1 min during setting on a TEM.

EELS spectra were measured using an energy filter (GIF Model 678, Gatan Inc.) attached on a TEM (CM200FEG, FEI Company). The TEM was equipped with a field emission gun and operated at an acceleration voltage of 200 kV. Spectra were recorded with a parallel detector in a range of about 100 eV with an interval of 0.1 eV. Energy loss was calibrated so that the peak energy of the Ni L_3 edge of NiO is 854 eV. Backgrounds were fitted to exponential functions in prepeak regions and were subtracted from the measured spectra. Energy resolution ranged from 0.8 to 1.0 eV in a full width at half-maximum of a zero-loss peak.

Results and Discussion

Characterization of $LiNiO_2$. The $LiNiO_2$ sample was characterized both by XRD and charge-discharge cycle tests to examine its quality. Figure 3 shows the XRD pattern of the sample. All diffraction peaks are indexed to an α-$NaFeO_2$ structure with a space-group symmetry of $R\bar{3}m$. There is no evidence to show crystalline impurity phases. Lattice constants were evaluated to be 2.876 Å for *a*-axis and 14.180 Å for *c*-axis in a hexagonal setting by a least-squares method with angles of the major 10 peaks. These values are consistent with literature.[24] Figure 4 shows the voltage curves of the initial three cycles for the nonaqueous lithium cell consisting of the $LiNiO_2$ composite electrode. The first cycle charge capacity was 260 $mAh{\cdot}g^{-1}$ by weight of $LiNiO_2$, and this value is 95% of the theoretical capacity for complete lithium extraction. The first cycle discharge capacity was 218 $mAh{\cdot}g^{-1}$. The large irreversible capacity in the first cycle is a typical characteristic of $LiNiO_2$ as discussed in the literature.[25,26] The cell showed good reversibility with a capacity of more than 200 $mAh{\cdot}g^{-1}$ in the following cycles.

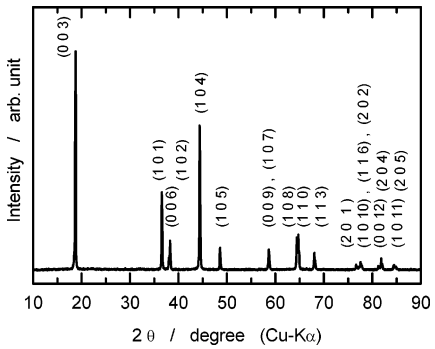

Figure 3. X-ray diffraction pattern of the $LiNiO_2$ sample. Peaks are indexed with a hexagonal cell.

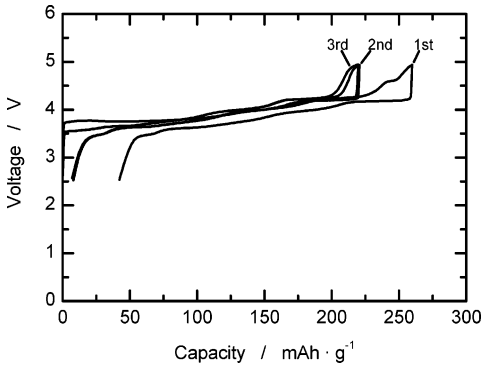

Figure 4. Voltage curves of the initial three cycles for a nonaqueous lithium cell of a $LiNiO_2$ composite electrode.

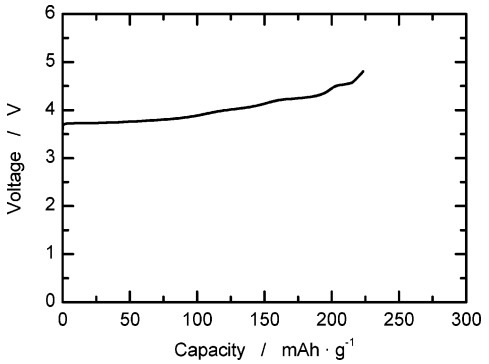

Figure 5. Voltage curve for charging a $LiNiO_2$ pellet electrode.

The XRD pattern and charge-discharge cycle tests indicate that the prepared $LiNiO_2$ sample is suitable as an electrode material. Hence, EELS measurements on the sample are worthwhile. The voltage curves show that most of lithium in the sample can be extracted when lithium cells are charged up to 5.0 V. Consequently, an electrochemical method was adopted to prepare NiO_2 for EELS measurements.

Preparation of NiO_2. A lithium cell consisting of a $LiNiO_2$ pellet as a positive electrode was charged up to 5.0 V to prepare NiO_2 for EELS measurements. The voltage curve of the cell is illustrated in Figure 5. The capacity of the charging was 223 $mAh{\cdot}g^{-1}$ which corresponds to 81% of the theoretical value of $LiNiO_2$. Although the capacity of the $LiNiO_2$ pellet was clearly

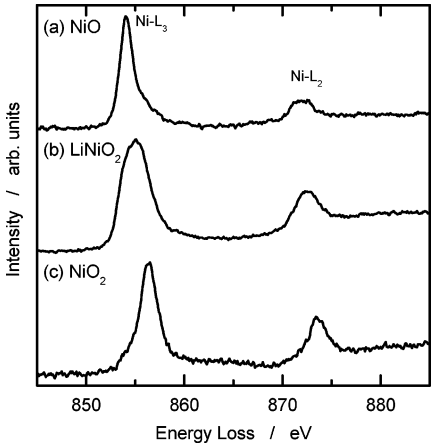

Figure 6. Ni $L_{2,3}$ edge ELNES of (a) NiO, (b) $LiNiO_2$, and (c) NiO_2. Each spectrum is normalized by the maximum intensity.

smaller than that of the $LiNiO_2$ composite electrode shown in Figure 4, the shape of the voltage curve was similar. Consequently, it is reasonable to consider that a part of the pellet was available as an active material and lithium was extracted from the active part up to the same level as in the case of the $LiNiO_2$ composite electrode. In this case, individual particles can be distinguished as active or not by Li K edge ELNES as shown and discussed later. Chemical analysis was not done to estimate the amount of the residual lithium in the sample, since it can provide only average composition of the sample. The sample will be called NiO_2 hereafter for simplicity.

Ni $L_{2,3}$ Edge ELNES. ELNES originates from electron transitions from core levels to unoccupied states. The transitions approximately follow the electric-dipole selection rule. Since the electronic structure of Ni-3d orbitals is the most interesting for the solid-state redox reaction of $LiNiO_2$, ELNES at Ni $L_{2,3}$ edge was measured for NiO, $LiNiO_2$, and NiO_2. Figure 6a shows the Ni $L_{2,3}$ edge ELNES of NiO. Spin-orbit coupling dissolves degeneracy on Ni-2p orbitals into doubly degenerated $2p_{1/2}$ with a lower energy and quadruple $2p_{3/2}$ with a higher energy. Consequently, the Ni $L_{2,3}$ edge ELNES consists of two major peaks associated with transitions from $2p_{1/2}$ orbitals (L_2 edge around 870 eV) and those from $2p_{3/2}$ (L_3 edge around 855 eV). Although the electric-dipole selection rule also allows transitions from Ni-2p levels to Ni-4s orbitals, transition probability to Ni-4s is much smaller than that to Ni-3d. Hence, the transitions to Ni-4s can be disregarded in the discussion on the Ni $L_{2,3}$ edge ELNES. The observed L_3 peak at 854 eV was sharp with a shoulder toward higher energy, and the L_2 peak at 872 eV was trapezoidal-shaped. Ni $L_{2,3}$ edge NEXAFS of NiO has been reported with a higher energy resolution.[18] According to the literature, minor peaks are hidden in the shoulder of the L_3 peak in Figure 6a and the trapezoidal-shaped L_2 peak consists of a doublet. Energy resolution of the ELNES in the present work is high enough to discuss major features, but it is not for minor ones.

Figure 6b shows the Ni $L_{2,3}$ edge ELNES of $LiNiO_2$. It has a broad L_3 peak at 855 eV and a triangular-shaped L_2 peak at 873 eV. These features are clearly different from those of NiO. Since Ni-3d orbitals are localized on a nickel atom, the shape of the Ni $L_{2,3}$ edge ELNES strongly reflects the local electronic structure of the nickel atom, for example, oxidation number, spin state, and coordination number. The different features of the Ni $L_{2,3}$ edge ELNES, therefore, suggest that the nickel atoms are in a different electronic structure in $LiNiO_2$ from those in NiO. The Ni $L_{2,3}$ edge ELNES of NiO_2 illustrated in Figure 6c

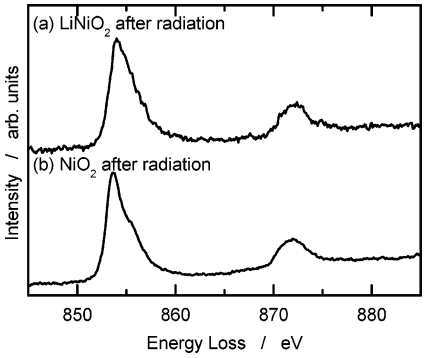

Figure 7. Ni $L_{2,3}$ edge ELNES of (a) $LiNiO_2$ after 10 min of radiation by an electron beam and (b) NiO_2 after 5 min of radiation. Each spectrum is normalized by the maximum intensity.

has different features than either NiO or $LiNiO_2$. The L_3 peak of NiO_2 at 857 eV is sharp like that of NiO, but it does not have a shoulder on the higher energy side. The L_2 peak of NiO_2 is triangular-shaped at 874 eV like that of $LiNiO_2$. Accordingly, the electronic structure of the nickel atoms in NiO_2 is not similar to that in either NiO or $LiNiO_2$.

The Ni $L_{2,3}$ edge NEXAFS of $LiNiO_2$ has already been reported.[18,19] The Ni $L_{2,3}$ edge spectrum of $LiNiO_2$ was determined to be similar to that of NiO in the literature. Contrary to the literature, the Ni $L_{2,3}$ edge ELNES of $LiNiO_2$ is clearly different than that of NiO in the present work. Readers may think that the electron beam may have damaged the samples during the measurements in the present work and that the radiation damage brings about the differences in the spectral shape. The following measurements were done to examine the effect of the radiation damage. The samples of $LiNiO_2$ and NiO_2 were left under a concentrated electron beam after the first measurements that are shown in Figure 6. Then, ELNES were recorded intermittently. Change in Ni $L_{2,3}$ edge ELNES was clearly seen for both $LiNiO_2$ and NiO_2. A new peak appeared at ~854 eV, on the lower energy side of the L_3 peak, and it grew up with exposure to the beam. The energy of the new peak is almost the same as that of the L_3 peak for NiO. Eventually, the spectra of both $LiNiO_2$ and NiO_2 became similar to that of NiO after a long-time irradiation. Figure 7 shows the spectrum of $LiNiO_2$ after 10 min of irradiation and that of NiO_2 after 5 min. The L_3 edge, having two peaks at ~854 and ~856 eV, was occasionally observed for both $LiNiO_2$ and NiO_2 even though the spectra were quickly measured. Consequently, the electron beam can definitely damage $LiNiO_2$ and NiO_2, and the radiation damage leads to nickel atoms in a similar electronic structure to that in NiO. The spectra shown in Figure 6b and 6c were, however, recorded as soon as the particles came into the view of the TEM, and no peak is apparent at 854 eV. Spectra of $LiNiO_2$ and NiO_2 at other edges, which will be shown in the following sections, were also recorded very quickly. Hence, the authors confirmed that the radiation damage did not affect the spectra in the present work. It can be suspected that the reported NEXAFS dominantly shows the electronic structure at the surface, not for the bulk, which should be the reason for the difference between the spectra in the present work and those in the literature. The surface effect has also been reported by Abraham et al. in NEXAFS and ELNES measurements on $LiNiO_2$ and $LiCo_{0.2}Ni_{0.8}O_2$.[17]

The different spectral shape in Figure 6 can be ascribed to the different formal charge of the nickel atoms among the three phases. This can be supported by first-principles calculations. Theoretical calculations beyond the one-electron approximation is necessary for Ni $L_{2,3}$ edge ELNES to take account of strong

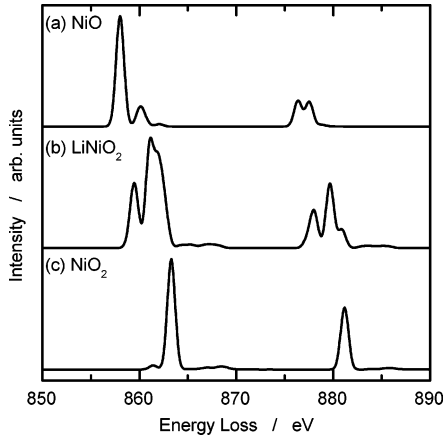

Figure 8. Theoretical Ni $L_{2,3}$ edge ELNES of (a) NiO, (b) $LiNiO_2$, (c) and NiO_2 by the first-principles method (ref 28).

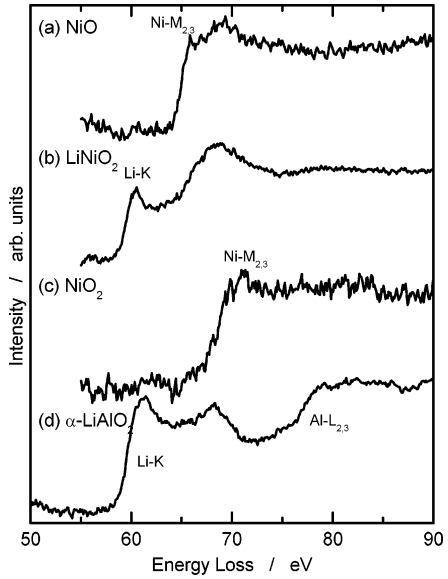

Figure 9. Ni $M_{2,3}$ and Li K edge ELNES of (a) NiO, (b) $LiNiO_2$, (c) NiO_2, and (d) α-$LiAlO_2$ (Li K and Al $L_{2,3}$ edge ELNES). Each spectrum is normalized by the maximum intensity.

correlation among the electrons on the Ni-3d orbitals and the hole on the Ni-2p. This kind of calculation is, however, not common even today. Figure 8 shows theoretical Ni $L_{2,3}$ edge ELNES of NiO, $LiNiO_2$, and NiO_2 by a novel calculation technique developed in the authors' group. Computational details can be found in refs 27 and 28. The calculation results reproduce the characteristics of the spectra as well as the chemical shifts. The results also show that the ground state of the nickel atoms is Ni^{2+} in NiO, Ni^{3+} with a low-spin state in $LiNiO_2$, and Ni^{4+} with a low-spin state in NiO_2, in the formal sense. Hence, it can be concluded that the formal charges of the nickel atoms are well described by the conventional chemical idea and this is consistent with the calculated electronic structures shown in Figure 1.

Ni $M_{2,3}$ and Li K Edge ELNES. Ni $M_{2,3}$ edge ELNES was measured for NiO, $LiNiO_2$, and NiO_2 as illustrated in Figure 9. Since Ni $M_{2,3}$ edge ELNES is a result of electron transitions from Ni-3p orbitals to unoccupied Ni-3d ones, it can be expected to provide additional information on the electronic structure of the Ni-3d orbitals. The Ni $M_{2,3}$ edge ELNES of NiO (Figure 9a) has an edge at 65 eV. Clear separation between the Ni M_2 and M_3 edges cannot be seen, because the spin-orbit coupling on Ni-3p orbitals is much weaker than that on Ni-2p. The

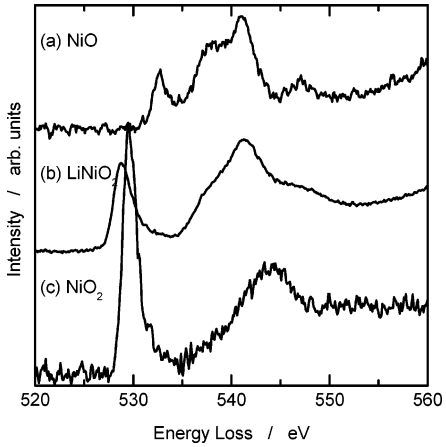

Figure 10. O K edge ELNES of (a) NiO, (b) $LiNiO_2$, and (c) NiO_2. Each spectrum is normalized by the maximum intensity in a range of 535−560 eV.

ELNES of $LiNiO_2$ (Figure 9b) has a Li K edge at 60 eV and two major peaks at 61 and 69 eV. The former peak would belong to the Li K edge and not to the Ni $M_{2,3}$.[22,29] However, it is not clear if the later peak at 69 eV belongs to only the Ni $M_{2,3}$ edge or both the Li K and Ni $M_{2,3}$. Li K edge ELNES of α-$LiAlO_2$, which has the same crystal structure as $LiNiO_2$, was measured and illustrated in Figure 9d to examine the shape of Li K edge ELNES. It is easier to examine the spectral shape of the Li K edge with α-$LiAlO_2$ than with $LiNiO_2$, because Al $L_{2,3}$ edge is higher in energy than Ni $M_{2,3}$. The spectrum of α-$LiAlO_2$ has two edges, Li K edge at 60 eV and Al $L_{2,3}$ at 77 eV. There are two peaks belonging to the Li K edge at 61 and 68 eV. Accordingly, the peak at 69 eV in the ELNES of $LiNiO_2$ should be a superposition of the Li K and Ni $M_{2,3}$ edges. It is difficult to discuss the local electronic structure of the nickel atoms in $LiNiO_2$ from the Ni $M_{2,3}$ edge ELNES. The Ni $M_{2,3}$ edge ELNES of NiO_2 shown in Figure 9c has an edge at 69 eV and no notable peak can be found at ~60 eV. Although many particles in the TEM were examined to find residual lithium, none of them showed a detectable strength of a Li K edge peak. This confirms that the NiO_2 sample in the present work is rather uniform in chemical composition and contains no detectable lithium. The energy of the Ni $M_{2,3}$ edge in NiO_2 is approximately 3 eV higher than that in NiO, which is a similar magnitude of the shift to that of Ni L_2 and L_3 peaks as described in the previous section. The Ni $M_{2,3}$ edge ELNES also supports the electronic structure of the nickel atoms as described in the previous section.

O K Edge ELNES. The electronic structure of oxygen atoms will be discussed in this section by O K edge ELNES. O K edge ELNES mainly corresponds to electron transitions from O-1s core level to unoccupied O-2p orbitals. Although the O-2p orbitals are filled in oxides in the formal sense, the transitions can take place via covalent bonding among the oxygen atoms and cations, as can be seen in Figure 10. The ELNES of NiO (Figure 10a) consists of four major peaks at 532, 538, 541, and 547 eV. The O K edge ELNES of NiO has been analyzed by first-principles calculations.[30] The first peak corresponds to transitions to the band mainly consisting of Ni-3d orbitals, which is labeled as Ni-$e_g\downarrow$ in Figure 1a. The other peaks at 535−550 eV correspond to transitions to the Ni-4sp band. The ELNES of $LiNiO_2$ (Figure 10b) also consists of four major peaks. The first peak is notably lower in energy and greater in intensity than that in NiO. In contrast to the clear differences for the first peak, the other peaks at 535−550 eV show only minor changes in both energy and intensity. The O K edge ELNES of

NiO_2 in Figure 10c consists of two major peaks at 530 and 544 eV. The first peak is located at a slightly higher energy than that for $LiNiO_2$, and its intensity is much greater. The energy of the second peak is also higher than that of the strongest peak for either NiO or $LiNiO_2$. The increased signal-to-background ratio for NiO_2 as compared with the other two is due to the very quick measurement to avoid the radiation damage as already discussed.

The first peak at ~530 eV remarkably becomes greater in intensity in the order NiO, $LiNiO_2$, and NiO_2, although the number of unoccupied Ni-3d orbitals per an oxygen atom does not change so much: It is 2 for an oxygen atom in NiO (Ni^{2+}:d^8), 1.5 (three orbitals for two oxygen atoms) in $LiNiO_2$ (Ni^{3+}:d^7), and 2 (four for two) in NiO_2 (Ni^{4+}:d^6). Because the electron transitions corresponding to the first peak take place via covalent bonding between the O-2p and Ni-3d orbitals, the intensity of the first peak indicates that the covalent bonding becomes stronger in the order NiO, $LiNiO_2$, and NiO_2. This is consistent with the calculation results that show greater contribution of O-2p orbitals in the Ni-3d band in the same order as shown in Figure 1. Although the intensity of the first peak changes monotonically, peak energies are not the case. NiO and $LiNiO_2$ have different energies for the first peak, but they have a similar energy and intensity for the other peaks at 535−550 eV. This is well consistent with the theoretical results shown in Figure 1. The energy between the Ni-$e_g\downarrow$ and Ni-4sp/Li-2sp bands is larger in $LiNiO_2$ than that in NiO. Since the Ni-4sp/Li-2sp band is delocalized, a similar spectral shape in the range of 535−550 eV suggests little difference in the electronic structure of the oxygen atoms in NiO and $LiNiO_2$. The difference in energy of the first peak would be basically due to the formal charge of the nickel atoms: Ni^{2+} in NiO versus Ni^{3+} with a low-spin state in $LiNiO_2$. NiO_2 has a larger difference in energy between the first and second peaks than $LiNiO_2$, as predicted by the first-principles calculations. The higher energy of both of the peaks in NiO_2 with respect to those in $LiNiO_2$ suggests a shift of the whole O K edge spectrum toward higher energy. The shift would be caused by the reduction in electron density at the oxygen atoms as shown in Figure 2. Although the redox center of $LiNiO_2$ is not oxygen but nickel as shown by the Ni $L_{2,3}$ edge ELNES, the oxidation of the nickel atoms makes covalent bonding between the nickel and oxygen atoms much stronger, leading to a reduction in electron density at the oxygen atoms. The whole O K edge spectrum can thereby shift toward higher energy.

Summary: Electronic Structure of Lithium Nickel Oxides. The electronic structures of NiO, $LiNiO_2$, and NiO_2 have been investigated by the electon energy loss spectroscopy at Ni $L_{2,3}$, Ni $M_{2,3}$, and O K edges. The ELNES at both Ni $L_{2,3}$ and $M_{2,3}$ edges indicate that nickel atoms have different formal charges among the three phases: Ni^{2+} in NiO, Ni^{3+} with a low-spin state in $LiNiO_2$, and Ni^{4+} with a low-spin state in NiO_2. This means that the redox center of $LiNiO_2$ to NiO_2 is nickel, as the conventional chemical idea has described. In contrast to the conventional idea, O K edge ELNES suggests that lithium extraction from $LiNiO_2$ remarkably changes the electronic structure of the oxygen atoms. The suggested electronic structures of the three phases are schematically illustrated in Figure 11. The basic electronic structure is similar between NiO and $LiNiO_2$ except for the Ni-3d band. The Ni-3d band becomes lower in energy and the contribution of O-2p orbitals in the Ni-3d band becomes greater with the increase of the formal charge of the nickel atoms from NiO to $LiNiO_2$. This makes the first peak of the O K edge ELNES lower in energy and greater in intensity for $LiNiO_2$ than NiO. Lithium extraction to NiO_2 causes the same changes for the Ni-3d band. In addition to the changes, the covalent bonding between the oxygen and nickel atoms is reinforced. This reduces electron density at the oxygen atoms, leading to a shift of O-1s core level downward. The shift of O-1s level cancels the change in energy of the Ni-3d band, which results in the slightly higher energy of the first peak for NiO_2 than for $LiNiO_2$. The shift also leads to the larger transition energy to the Ni-4sp band, which is observed as the shift of the peak at 544 eV. The change in the electronic structure of the oxygen atoms by the lithium extraction is so remarkable that O K edge ELNES shows the chemical shift toward higher energy for NiO_2. The difference in the electronic structure of the oxygen atoms between NiO and $LiNiO_2$ is not so significant, since no chemical shift can be observed in O K edge ELNES.

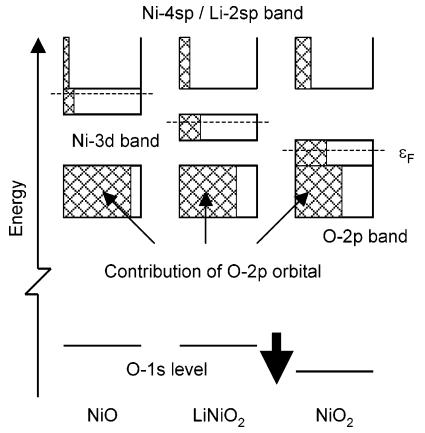

Figure 11. Schematic electronic structures of (a) NiO, (b) $LiNiO_2$, and (c) NiO_2. Contribution of O-2p orbital is denoted by cross-patterned areas.

Acknowledgment. The authors are grateful to Professor Tsutomu Ohzuku of Osaka City University (OCU) in Japan for his help in sample preparation and encouraging discussion. The present work is supported by grant-in-aids for scientific research from the Ministry of Education, Culture, Sports, Science, and Technology (MEXT) of Japan. Authors (Y. K., T. M., and H. I.) thank the Japan Society for the Promotion of Science (JSPS) for their research fellowship.

References and Notes

(1) Miura, K.; Yamada, A.; Tanaka, M. *Electrochim. Acta* **1996**, *41*, 249.
(2) Ceder, G.; Aydinol, M. K.; Kohan, A. F. *Comput. Mater. Sci.* **1997**, *8*, 161.
(3) Aydinol, M. K.; Kohan, A. F.; Ceder, G.; Cho, K.; Joannopoulos, J. *Phys. Rev. B* **1997**, *56*, 1354.
(4) Deiss, E.; Wokaun, A.; Barras, J.-L.; Daul, C.; Dufek, P. *J. Electrochem. Soc.* **1997**, *144*, 3877.
(5) Aydinol, M. K.; Ceder, G. *J. Electrochem. Soc.* **1997**, *144*, 3832.
(6) Wolverton, C.; Zunger, A. *Phys. Rev. B* **1998**, *57*, 2242.
(7) Wolverton, C.; Zunger, A. *Phys. Rev. Lett.* **1998**, *81*, 606.
(8) Van der Ven, A.; Aydinol, M. K.; Ceder, G.; Kresse, G.; Hafner, J. *Phys. Rev. B* **1998**, *58*, 2975.
(9) Mishra, S. K.; Ceder, G. *Phys. Rev. B* **1999**, *59*, 6120.
(10) Koyama, Y.; Kim, Y.-S.; Tanaka, I.; Adachi, H. *Jpn. J. Appl. Phys.* **1999**, *38*, 2024.
(11) Grechnev, G. E.; Ahuja, R.; Johansson, B.; Eriksson, O. *Phys. Rev. B* **2002**, *65*, 174408.
(12) Koyama, Y.; Yabuuchi, N.; Tanaka, I.; Adachi, H.; Ohzuku, T. *J. Electrochem. Soc.* **2004**, *151*, A1545.
(13) Pickering, I. J.; George, G. N.; Lewandowski, J. T.; Jacobson, A. *J. Am. Chem. Soc.* **1993**, *115*, 4137.
(14) Rougier, A.; Delmas, C. *Solid State Commun.* **1995**, *94*, 123.

(15) Nakai, I.; Takahashi, K.; Shiraishi, Y.; Nakagome, T.; Izumi, F.; Ishii, Y.; Nishikawa, F.; Konishi, T. *J. Power Sources* **1997**, *68*, 536.

(16) Mansour, A. N.; Yang, X. Q.; Sun, X.; McBreen, J.; Croguennec, L.; Delmas, C. *J. Electrochem. Soc.* **2000**, *147*, 2104.

(17) Abraham, D. P.; Twesten, R. D.; Balasubramanian, M.; Kropf, J.; Fischer, D.; McBreen, J.; Petrov, I.; Amine, K. *J. Electrochem. Soc.* **2003**, *150*, A1450.

(18) Montoro, L. A.; Abbate, M.; Almeida, E. C.; Rosolen, J. M. *Chem. Phys. Lett.* **1999**, *309*, 14.

(19) Uchimoto, Y.; Sawada, H.; Yao, T. *J. Power Souces* **2001**, *97*−*98*, 326.

(20) Shiraishi, Y.; Nakai, I.; Kimoto, K.; Matsui, Y. *J. Power Sources* **2001**, *97*−*98*, 461.

(21) Graetz, J.; Hightower, A.; Ahn, C. C.; Yazami, R.; Rez, P.; Fultz, B. *J. Phys. Chem. B* **2002**, *106*, 1286.

(22) Graetz, J.; Ahn, C. C.; Yazami, R.; Fultz, B. *J. Phys. Chem. B* **2003**, *107*, 2887.

(23) Blaha, P.; Schwarz, K.; Madsen, G.; Kvasnicka, D.; Luitz, J. *WINE2k, An Augmented Plane Wave Plus Local Orbitals Program for Calculating Crystal Properties*; Vienna University of Technology: Vienna, Austria, 2001.

(24) Ohzuku, T.; Ueda, A.; Nagayama, M. *J. Electrochem. Soc.* **1993**, *140*, 1862.

(25) Peres, J. P.; Delmas, C.; Rougier, A.; Broussely, M.; Perton, F.; Biensan, P.; Willmann, P. *J. Phys. Chem. Solids* **1996**, *57*, 1057.

(26) Arai, H.; Okada, S.; Sakurai, Y.; Yamaki, J. *Solid State Ionics* **1997**, *95*, 275.

(27) Ogasawara, K.; Iwata, T.; Koyama, Y.; Ishii, T.; Tanaka, I.; Adachi, H. *Phys. Rev. B* **2001**, *64*, 115413.

(28) Ikeno, H.; Tanaka, I.; Koyama, Y.; Mizoguchi, T.; Ogasawara, K. *Phys. Rev. B*, submitted.

(29) Tsuji, J.; Nakamatsu, H.; Mukoyama, T.; Kojima, K.; Ikeda, S.; Taniguchi, K. *X-Ray Spectrom.* **2002**, *31*, 319.

(30) Kanda, H.; Yoshiya, M.; Oba, F.; Ogasawara, K.; Adachi, H.; Tanaka, I. *Phys. Rev. B* **1998**, *58*, 9693.